The International Journal of Advanced Manufacturing Technology (2018) 96:4085–4094
https://doi.org/10.1007/s00170-018-1828-x

ORIGINAL ARTICLE

Experimental and numerical assessment of mechanical properties of thin-walled aluminum parts produced by liquid impact forming

Javad Shahbazi Karami[1] · Seyed Davoud Nourbakhsh[2] · Kian Tafazzoli Aghvami[2]

Received: 16 February 2017 / Accepted: 20 February 2018 / Published online: 17 March 2018

Abstract
Quick, low-cost, and high-quality manufacturing is considered a key factor in today's industry. Therefore, researchers have turned to inventing new methods and technologies for meeting such industrial requirements. Liquid impact forming is one such method which is being increasingly developed in different industries, such as automotive and aerospace. Considered to be a tube hydroforming process, this forming method utilizes liquid pressure to produce the desired shape. In this study, the liquid impact forming process, which was applied to a thin-walled tube made of 6063 aluminum alloy, was experimentally and numerically investigated. In the experimental section, a new die was designed and manufactured for deforming the cross section of the aluminum tube into a hexagonal profile. To investigate the characteristics of the hexagonal profile obtained from the forming process, tensile and three-point bend tests were performed. According to the results obtained from the tensile test, the tensile yield strength in the workpiece increased by 21 MPa due to work hardening. The results obtained from the three-point bend test indicated that the flexural strength of the circular tube was greater than that of the hexagonal profile due to its greater moment of inertia. The numerical results included plastic equivalent strain distribution, variations in the profile thickness, and the force required for the forming process. Upon comparing the workpiece thicknesses obtained from numerical simulation and measurements, a good agreement was observed.

Keywords Tube hydroforming · Liquid impact forming · Finite element simulation · Tensile test · Bend test · 6063 aluminum alloy

1 Introduction

Hydroforming has been a major metal forming process since before World War II. This process has witnessed significant growth since the 1990s, particularly in automotive industry applications [1]. Due to its prominent characteristics, hydroforming process is used for producing components in aerospace and automotive industries [2]. When compared to other metal forming methods, hydroforming offers significant advantages, including higher production repeatability, lower cost, less component weight, improved structural strength, and fewer requirements in terms of secondary operations and processes [3].

Considering its advantages, hydroforming is used to form tubes on a large scale. In this process, high-pressure fluids, such as water, are used to create various forms of tubes. Tube hydroforming processes include four methods, namely liquid impact forming (LIF), hot forming (HF), low-pressure hydroforming (LPH), and high-pressure hydroforming (HPH) [4].

In LIF process, the desired form of the workpiece is obtained using stamping press and liquid pressure. In this process, the tube is filled with liquid, and then both ends become sealed and stamped at a specified point. Water is the frequently used liquid, which serves to form and support the tube. The distinction between liquid impact forming and conventional hydroforming is that the former utilizes stamping press instead of hydraulic one, which is commonly used in hydroforming. In contrast to conventional hydroforming, LIF process does not require water injection or compression of tube length. In this process, deformation depends on the tension applied to the test tube as well as its material and thickness. In addition,

✉ Kian Tafazzoli Aghvami
k_tafazoli@mecheng.iust.ac.ir

[1] Faculty of Mechanical Engineering, Shahid Rajaee Teacher Training University (SRTTU), Shabanlou St., Lavizan, P.O. Box 16785-136, Tehran 1678815811, Iran

[2] School of Mechanical Engineering, Iran University of Science and Technology, Hengam St., Resalat Sq., P.O. Box 16765-163, Tehran 1684613114, Iran

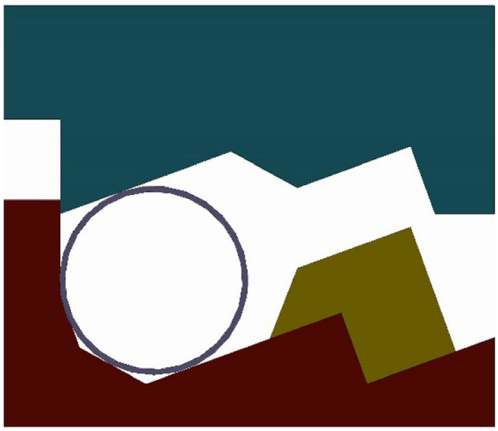

Fig. 1 Liquid impact forming die

shorter cycle times (about 8–15 s) contribute to making the process less expensive [4]. Hydroforming process requires accurate control of various conditions including internal pressure, closing of the die, and sealing [5].

In the low-pressure hydroforming method, pressure is maintained inside the tube which is formed by means of a punch or the movement of the upper die [6]. The required pressure is much lower in low-pressure hydroforming as compared to the high-pressure method.

Figure 1 shows a typical liquid impact forming die, in which the tube is initially filled with a specific liquid. Then, both ends are sealed and placed in the die. The forming process starts with the upper die moving downwards by the force of the press. As a result of this downward movement, the tube volume starts decreasing, leading to a consequent increase in the fluid pressure inside the tube. Thus, the desired forming process is accomplished.

Figure 2 shows the final stage of the liquid impact forming die operation. Upon applying the suitable pressure, the workpiece takes the form of the die.

The first liquid impact forming die was patented by Ash [7]. Green Wheel Tool and Die Manufacturing Company designed a liquid impact die capable of both deforming and shaping concave areas in the tube [8]. Nikhare et al. used the liquid impact forming process to deform a tube into a workpiece with a rectangular profile [9], while Huang et al. designed a die to form a tube into a workpiece with triangular cross section [10]. Their study concluded that the internal tube pressure and the force exerted on the die by the press play pivotal roles in the LIF process. Hajializadeh and Mashhadi conducted a numerical analysis on liquid impact forming process for an aluminum 6061-T6 tube. They implemented explicit finite element method on a sheet and a tube formed by LIF process. Their results were in good agreement with experimental results from other researchers [11]. Masoumi et al. presented a "developed stress-based forming limit diagram" to predict the necking phenomenon and subsequently used it in tube hydroforming. They also simulated this process using finite element method; the obtained results were in good agreement with the respective experimental ones [12]. Hosseinzadeh et al. proposed a new sheet hydroforming technique by combining standard hydroforming methods with the hydromechanical sheet forming method [13]. Manabe and Amino investigated the parameters influencing the distribution of wall thickness in hydroformed tubes, through finite element method and experiment [14]. They considered stress ratio, coefficient of friction, and anisotropic parameter in their study and concluded that in tube hydroforming, anisotropic property is one of the most influential parameters affecting the forming process. Koc and Altan presented analytical models for prediction of various phenomena that occur in hydroforming as well as internal pressure and axial force, and also verified them using experimental results [15]. The use of such models in combination with finite element method

Table 1 Properties of the tube used in liquid impact forming process

Young's modulus (GPa)	Tensile yield strength (MPa)	Ultimate tensile strength (MPa)	Density (kg/m^3)	Poisson's ratio
70	211	250	2800	0.3

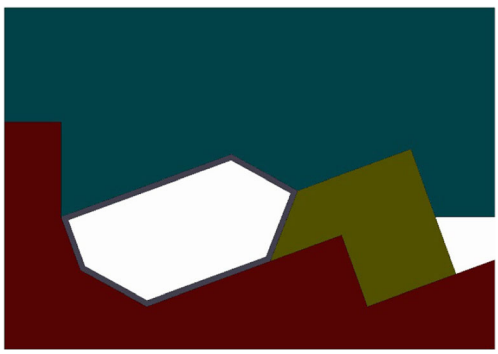

Fig. 2 The final form of liquid impact forming die

Fig. 3 The three-piece liquid impact forming die

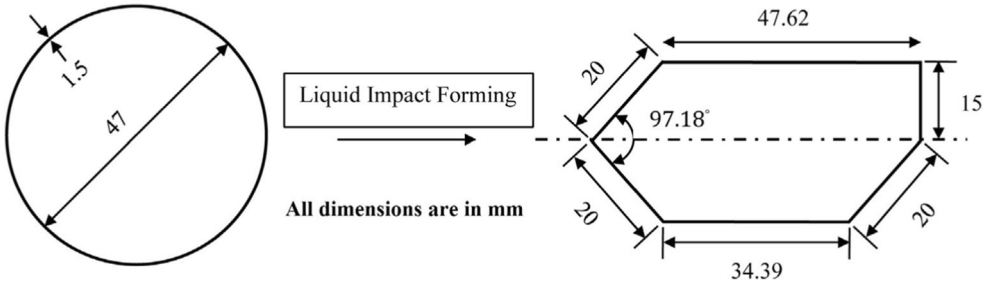

Fig. 4 The workpiece cross section

can offer a thorough understanding of this process. In another study, Trana conducted FE simulations of the hydroforming process for an automotive application [16]. He also considered preforming and bending for the entire process and showed that the bending operation and preforming are very important for the process conducted on this component. Shi et al. numerically simulated necking and fracture in tube hydroforming process and investigated the effect of pressure on necking and fracture initiation [17]. They found that the pressure has a great effect on the onset of fracture with the increase of pressure. Nikhare et al. proposed a method for estimating the minimum pressure required in the low-pressure hydroforming of a buckle-free component with sufficient accuracy [6].

In the present study, the liquid impact forming process applied to a thin-walled tube made of 6063 aluminum alloy is studied experimentally and numerically. The present study aims to design a new three-piece die capable of forming a complex shape without any external horizontal force and any external pressure increase during the forming process. In the experimental section, the main purpose is to design and manufacture a suitable die for deforming the tube cross section into a hexagonal profile using the LIF method. Moreover, the experimental section includes designing of a system for sealing the tube. Three different water pressures are applied and the corresponding results in each case are presented. In addition, the results obtained from tensile and bend tests are presented for investigating the mechanical properties of the workpiece. For the tensile test, these results include the engineering stress-strain diagrams. These diagrams are obtained for the deformed profile whose tensile yield strength is compared with the one obtained for the circular tube. For the bend test, the force-displacement diagrams obtained for the tube, before and after the deformation, are compared. In the numerical simulation section, the finite element method is used to analyze the LIF process by ABAQUS software. The simulation results including plastic equivalent strain distribution, obtained for the hexagonal profile, the workpiece thickness, and the force required for the forming process are presented. Additionally, the simulation results related to workpiece thickness are compared with those obtained from measurements.

2 Design and manufacture of the die

The liquid impact forming process was studied for converting the cross-sectional shape of a tube from a circle into a hexagon. Given the geometrical dimensions of the tube, the other components of the forming system can be designed. The tube, whose properties are shown in Table 1, was 25 cm in length and made of 6063 aluminum. Its external diameter and thickness were 50 and 1.5 mm respectively.

As shown in Fig. 3, the designed die comprises three parts: a fixed, a moving, and a sliding part. As the slide is located on a sloped surface, it moves more slowly than the upper die. This difference in speed causes the tube body to move towards the slide during the forming operation as a result of the clearance formed near the slide. At the end of the forming process, the slide gently pushes this volume into the die, thus leading to more exact forming of the workpiece corners. The sloped surface makes an angle of 20° with the horizontal, and the slide moves due to the applied force by the upper die. The die components are connected to the press by means of a 25×20 cm^2 shoe fitted with a 12.5-cm guide. The press is capable of exerting a maximum force of 600 kN.

During the liquid impact forming process, the aluminum tube is converted into a hexagonal profile with the specifications shown in Fig. 4.

The workpiece angles and sides are labeled, as observed in Fig. 5, in order to facilitate comparison of the different cases.

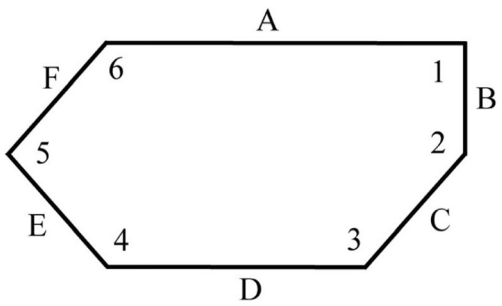

Fig. 5 Labeling the angles and sides of the workpiece

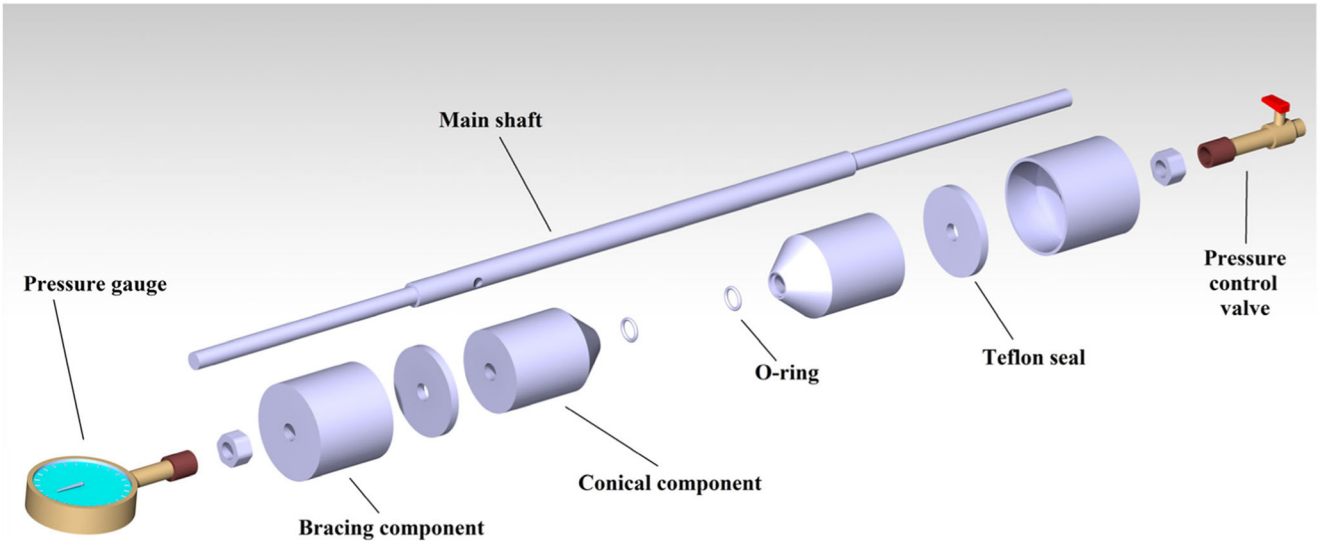

Fig. 6 Set of sealing assembly components

2.1 Manufacturing of the sealing assembly components

In the liquid impact forming method, the pressure of the fluid inside the tube is an important factor in the forming process. Sealing of the tube on both ends decreases the tube volume and consequently increases the internal fluid pressure. In the forming process, the cross section of the tube changes from a circle into a hexagon. The cross-sectional area of hexagon is less than that of circle with the same perimeter, while the length of the tube is the same in both cases. Therefore, the volume of the tube with a hexagonal cross section is less than that of the tube with a circular cross section. Since the fluid is incompressible, to avoid excessive pressure buildup inside the tube, the fluid must be guided outside the tube in a controlled manner. For this purpose, a controllable sealing system, shown schematically in Fig. 6, was designed comprising conical and bracing components, Teflon seal, the main shaft, a pressure gauge, and a control valve. The conical parts prevent sudden deformations at the outer edges of the die, which might lead to failure of the workpiece. The bracing component pushes the Teflon seal against the conical piece in order to prevent water penetration into the external parts. The main shaft connects the two braces by means of two nuts. As a result, the internal parts of the tube become fully sealed. The main shaft was designed as a tube with inner and outer diameters of 6 and 10 mm respectively. A 6-mm hole was drilled on either side of the main shaft, which is shown in Fig. 6, to connect it to the interior of the tube. Since the shaft is connected to the tube interior on both sides, a pressure gauge was placed at one end of the shaft and a control valve at the other end.

The pressure gauge was used for monitoring the pressure of the fluid inside the tube. The maximum pressure measured by this gauge was 10 MPa with the accuracy of ± 100 kPa.

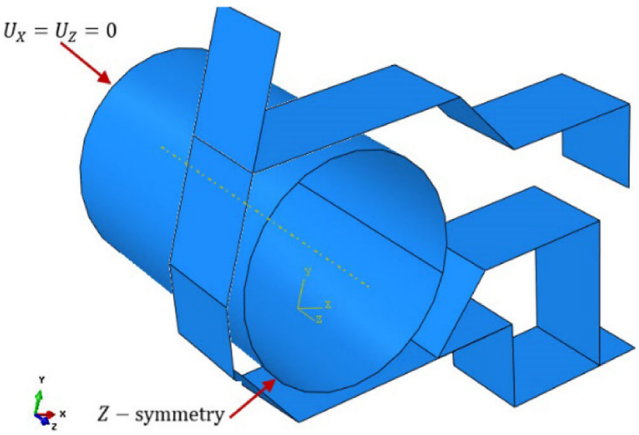

Fig. 7 Geometry of the die and the aluminum tube in ABAQUS software

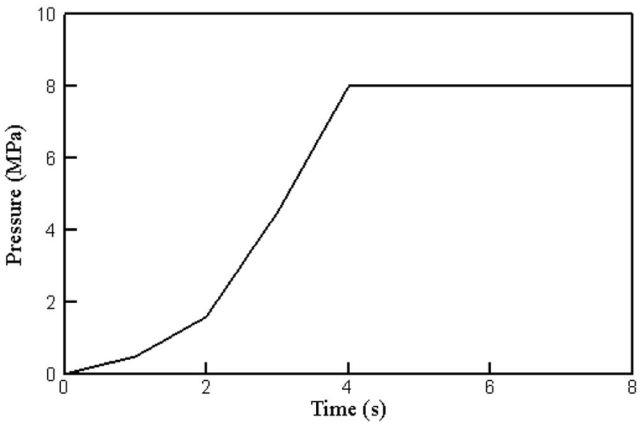

Fig. 8 Pressure variation with time

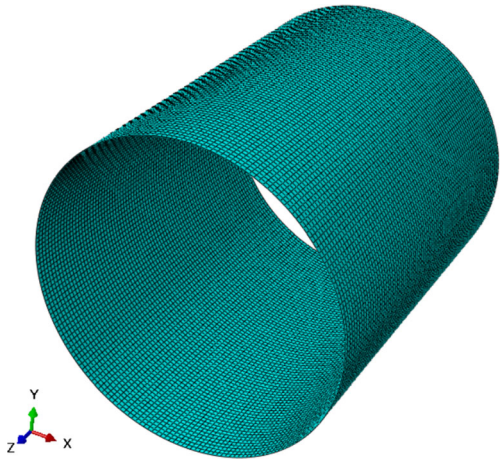

Fig. 9 Meshing of the aluminum tube in ABAQUS software

Reduction of the tube volume due to deformation causes pressure increase inside the tube, which necessitates expulsion of extra fluid volume so as to prevent the formation of cracks in the tube. In order to solve this problem, a pressure control valve was used, as shown schematically in Fig. 6 along with the pressure gauge. A groove was cut at the front of the conical part for fitting an O-ring to provide reliable sealing. As the shaft joins the two conical parts together, this O-ring is placed between the conical part and the shaft, thus preventing water from leaking out. In order to make the sealing more reliable, Teflon tape (thickness = 3 mm) was utilized between the brace and the conical piece, as shown in Fig. 6.

3 Experimental analysis

Tensile and bend tests were performed to study the mechanical properties of the samples produced by the liquid impact forming method as is explained below.

3.1 Tensile test

Tensile test is the most common test for determining mechanical properties, such as strength, ductility, toughness, and modulus of elasticity in a metal [1]. As shown in Fig. 5, tensile test specimens were prepared from all sides of the profile and subsequently tested in accordance with ASTM E8M standard test methods. The test apparatus was set to produce a vertical velocity of 1 mm/min during the experiment. The same conditions were considered for all the specimens.

Fig. 11 The test result for the tube filled with water at a pressure of 6 MPa using the three-piece die

3.2 Bend test

The three-point bend test was conducted on both the circular and the hexagonal profiles. Specimens used in the bend test were 25 cm long and the rate of displacement of the upper die was 1 mm/min for all the tests.

4 Finite element simulation

Numerical methods are powerful techniques used for analyzing metal forming processes, and the finite element (FE) method is one of the most efficient methods in this regard. In the FE method, all the conditions governing the problem can be used to closely approximate the actual conditions to produce acceptable solutions. ABAQUS software was used for simulation due to its various capabilities. Since the process to be simulated was similar throughout the tube, only one section of the tube, as well as the die, was simulated. Figure 7 demonstrates the geometry of the die and the tube assembly model in ABAQUS. As the tube thickness was negligible compared to the other tube dimensions, shell elements were used in modeling. The die to be analyzed had three parts, namely the moving, the fixed, and the sliding part, all of which were to be modeled and simulated. Die components were

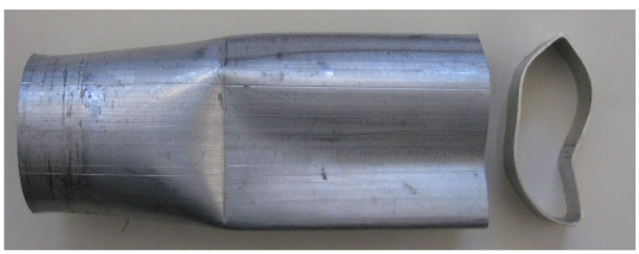

Fig. 10 The test result for empty tube using the three-piece die

Fig. 12 The test result for tube filled with water at a pressure of 7 MPa

Table 2 Comparison between the corner angles of the workpiece and the default case for the test at 7 MPa pressure

Corner no.	Workpiece angle (°)	Default case angle (°)	Difference (%)
1	87	90	−3.33
2	141.6	138.59	+2.17
3	134.1	131.41	+2.04
4	134.8	131.41	+2.58
5	99.2	97.18	+2.07
6	135.7	141.41	−4.03

Table 3 Comparison between the corner angles of the workpiece and the default case for the test at 8 MPa pressure

Corner no.	Workpiece angle (°)	Default case angle (°)	Difference (%)
1	87.5	90	−2.77
2	141	138.59	+1.73
3	132.5	131.41	+0.83
4	133	131.41	+1.21
5	98	97.18	+0.84
6	136.5	141.41	−3.47

considered as analytical rigid parts in the ABAQUS model. This type of rigid surface does not require meshing, thus expediting the simulation process. The displacement condition was assumed as the boundary condition for the moving part. The lower part was assumed to be fixed, and the slide was allowed to move upon contacting the upper die or the tube. The processes were similar at the other end of the tube; therefore, the tube was considered to be symmetrical at its other end.

As the pressure exerted onto the body by the fluid inside the tube is of particular importance in the liquid impact forming method, it was necessary to assume a pressure distribution along the body of the tube. The fluid pressure inside the aluminum tube was increasing with time. Figure 8 shows the pressure distribution applied in the simulation for the test where the pressure was 8 MPa. The coefficient of friction in the simulation was assumed to be 0.1 and surface-to-surface contact was considered between the relevant surfaces. The speed of the moving part was assumed to be 2.5 mm/s in the simulation based on the experimental conditions. Quad-Shell-S4R elements were selected for meshing the model, which is shown in Fig. 9. In order to check the independence of the results from the meshing, the number of elements was increased from 750 to 15,000. The results showed that increasing the number of elements led to a slow rate of increase in the corresponding forces applied to the die, and this rate was ultimately stabilized as the number of elements exceeded 10,000. For this reason, the number of elements in the tube model was set at 10,640. The properties of the aluminum tube in the simulation were calculated at 293.15 K in accordance with the actual conditions of the test location.

Fig. 13 The test result for the tube filled with water at a pressure of 8 MPa

5 Results and discussion

5.1 Results obtained from the forming process

In this section, the results obtained from the forming process are presented for two cases: (1) the case where no fluid was used and (2) the case where fluid was introduced in the test at pressures of 6, 7, and 8 MPa.

5.1.1 No fluid test

Figure 10 shows the results obtained from the forming process without any fluid being used. In this case, the

Fig. 14 Specimens at the end of the tensile test

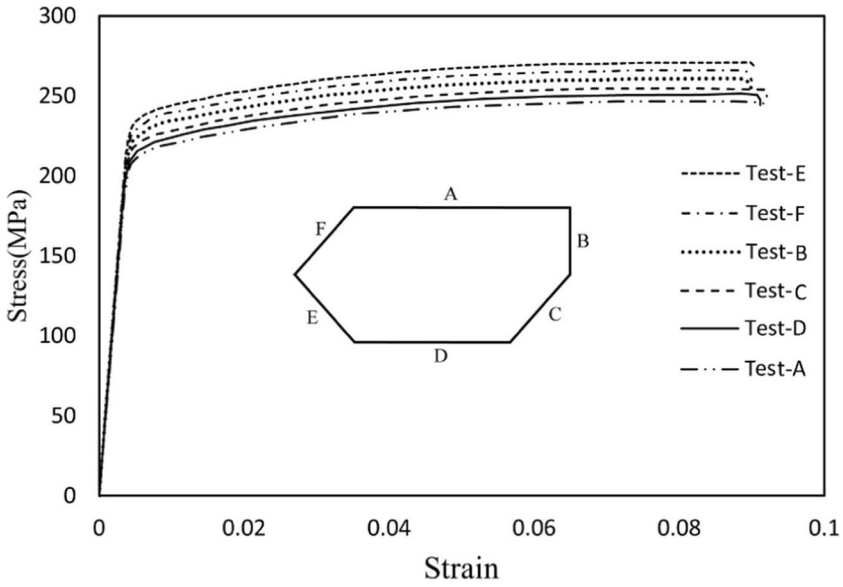

Fig. 15 Engineering stress-strain curves for specimens of the hexagonal profile

output shape of the profile was an irregular polygon with curves on its sides. These results revealed that this forming process required the application of a pressurized fluid.

5.1.2 Tests using fluid

For these tests, water was used as the fluid at pressures of 6, 7, and 8 MPa. Figure 11 shows the test results obtained at a water pressure of 6 MPa. In this test, the workpiece angles were not properly formed and the upper and lower sides of the workpiece were curved towards the interior of the shaft. Therefore, it can be concluded that the forming process could be improved by increasing the internal pressure in the tube.

The result of the same experiment at a pressure of 7 MPa is shown in Fig. 12. As can be observed, the curved sides of the workpiece have disappeared and the angles have a better form.

Table 2 compares the workpiece angles for the default case and those obtained from the workpiece for this test. As can be observed, corner no. 6 has not been properly formed yet, leading us to expect that a better form would be obtained upon a further increase in fluid pressure. The next test was conducted for improving the shape of workpiece corners, in which the tube pressure was assumed to be 8 MPa. Figure 13 shows the results obtained in this case, in which the corner shapes are greatly improved and can be accepted as the final results. Therefore, it is concluded that increasing the fluid pressure in the LIF process leads to better results. Table 3 compares the corner angles for the workpiece and the default case. As can be observed, the increase in pressure has a considerable effect on forming the corners.

5.2 Mechanical properties

5.2.1 Tensile test results

The results obtained from the tensile test are shown in Fig. 14. As can be observed, most specimens failed along the 45° direction, representing the state referred to as "ductile fracture."

As Fig. 15 demonstrates, each specimen has a different engineering stress-strain diagram. Such differences might be due to the difference in strain hardening that occurs during the forming process.

Table 4 shows the values of tensile yield strength, ultimate tensile strength, and modulus of elasticity for different specimens. Comparison with Table 1 indicates that the tensile yield strength in the workpiece during the liquid impact forming process was greater than that of the circular tube. The reason is that the polygon work-

Table 4 Values of tensile yield strength, ultimate tensile strength, and modulus of elasticity for the different specimens used in the tensile test

Modulus of elasticity (GPa)	Ultimate tensile strength (MPa)	Tensile yield strength (MPa)	Specimen
65	251	236	F
67	255	239	E
64.5	248	233	C
64	250	235	B
65	240	225	A
66	241	228	D

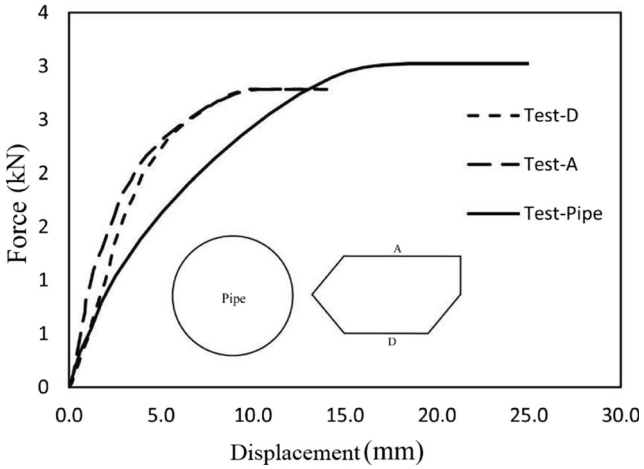

Fig. 16 Force variations with vertical displacement obtained from the bend test for the hexagonal profile (both layouts) and the circular tube

piece has experienced strain hardening as a result of the forming process. By calculating the average tensile yield strength of the samples obtained from the profile, it is concluded that its value has increased about 21 MPa as a result of work hardening in the workpiece. As Table 4 shows, the tensile yield strength values, which were obtained for different sides of the hexagon, were different, such that those sides which experienced greater deformation showed higher yield strength values. For example, specimens E and F were obtained from the sides with the greatest deformations, which had been formed at sharper angles as compared to the other specimens.

5.2.2 Three-point bend test results

Figure 16 shows the force-vertical displacement diagram obtained from the bend test for the hexagonal profile (in both layouts) and the circular tube. As can be observed, the circular tube has a greater flexural strength than the hexagonal profile. The reason is the greater area moment of inertia exhibited by the circular tube around the flexural axis.

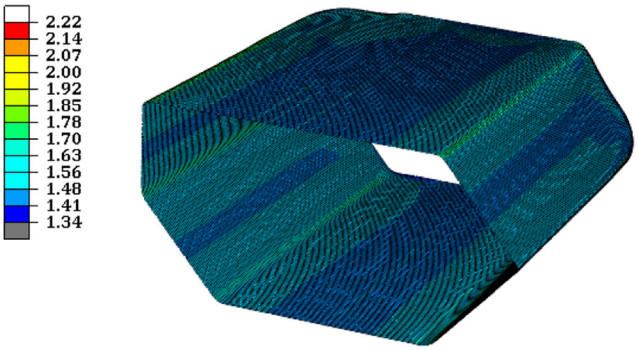

Fig. 18 Thickness distribution in the hydroformed tube (in mm)

5.3 Finite element simulation results

Numerical simulation of the liquid impact forming process was performed in ABAQUS software and the results related to plastic equivalent strain distribution, thickness variations, and the force required for the forming process were obtained. Figure 17 shows the distribution of plastic equivalent strain in the formed profile. As can be observed, the largest amounts of plastic equivalent strain occur at the corners of the workpiece, where the greatest deformation is observed. The test tube thickness in liquid impact forming process varies with liquid pressure and has a continuous distribution. As Fig. 18 shows, thickness has increased at the corners of the hydroformed tube.

The thickness distribution along the perimeter of the formed tube obtained from the finite element simulation is shown in Fig. 19. The origin was placed at corner 1 as shown in Fig. 5. A counterclockwise thickness distribution was assumed along the perimeter of the cross section of the formed tube (Fig. 5).

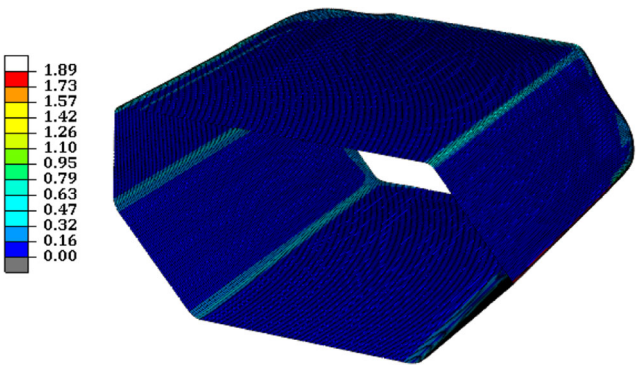

Fig. 17 Distribution of plastic equivalent strain

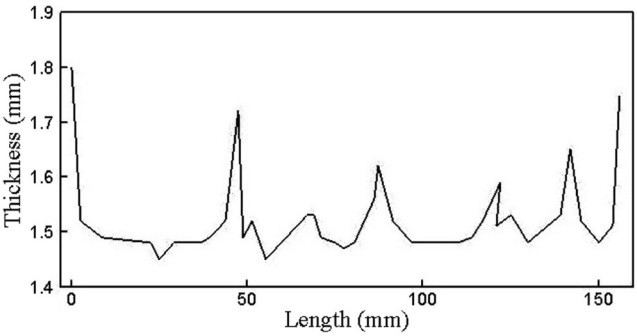

Fig. 19 Thickness distribution along the perimeter of the hydroformed tube

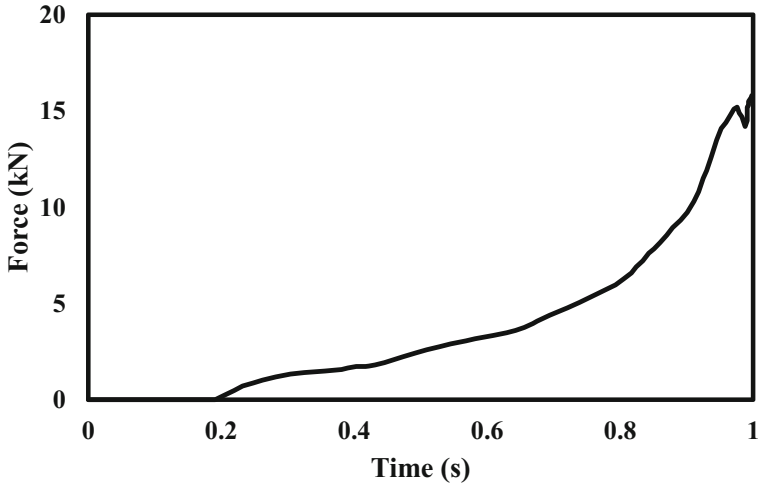

Fig. 20 Variations of the force exerted on the upper die with time

Figure 20 shows variations of the force exerted on the upper die with time. As time passed, the fluid pressure inside the tube increased, leading to a corresponding increase in the force applied to the die. On the other hand, the interface between the die and the tube body also increased with time.

5.4 Comparison between simulation and experimental results

In order to compare the simulation and experimental results, the workpiece was first cut with a wire-cutting machine and then the thicknesses were measured using a digital micrometer. The workpiece in this test was formed under a fluid pressure of 8 MPa. Figure 21 shows the results obtained for the thickness from simulation and measurement. As can be observed, the simulation results match the experimental measurements with acceptable accuracy. Based on the labeling method used in Fig. 5, the greatest thickness was obtained at corner 1 where a 12% increase was observed relative to the initial thickness at this corner.

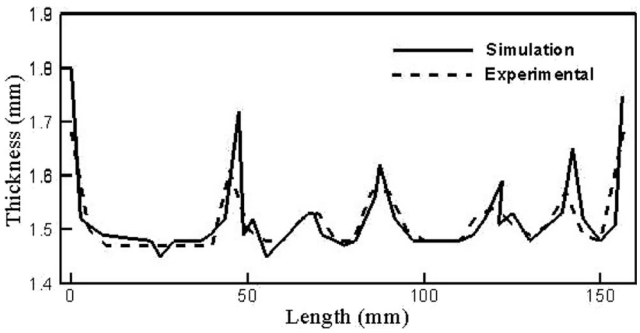

Fig. 21 Comparison between the thicknesses obtained from measurements and numerical simulation

6 Conclusions

This study compared the finite element simulation and the experimental results, which were obtained from the liquid impact forming process as applied to a thin-walled 6063 aluminum alloy tube. In the experimental section, a die comprising three components was designed and developed for deforming the tube profile from a circle into a hexagon. The tube was tested at three different fluid (i.e., water) pressures. The mechanical properties of the obtained profile were then studied through the tensile and the three-point bend tests. In the numerical simulation section, the results related to plastic equivalent strain distribution, thickness variations, and the force required for the forming process were obtained. The thicknesses obtained from the numerical simulation were then compared with experimental measurements. The following results were obtained from the experimental and numerical simulation methods:

1. As the fluid pressure was increased, the forming process generated better results; by increasing the pressure from 6 to 7 and ultimately to 8 MPa, the curvature at the sides of the profile disappeared and the corner angles took more favorable shapes, resulting in an almost desirable profile with more precise angles.
2. The tensile test results showed that the tensile yield strength of the profile obtained from the liquid impact forming process was about 21 MPa greater than that of the circular tube due to work hardening.
3. According to the plastic equivalent strain distribution in the hydroformed profile, obtained from FE simulation, the smaller the corner angle, the larger the amount of plastic deformation required to achieve the desired form. The angles which experienced the greatest deformation, according to Fig. 5, were angle nos. 1 and 5.

4. The profile thicknesses obtained from measurement and simulation for the workpiece formed through the test with 8 MPa pressure showed that thickness at the corners had increased and that a maximum thickness increase of 12% had resulted (as compared to the pre-test thickness).

Compliance with ethical standards

Conflict of interest The authors declare that they have no conflict of interest.

References

1. Zang SH (1999) Developments in hydroforming. J Mater Process Technol 91:236–244
2. Mohammadi F, Mashadi MM (2009) Determination of the loading path for tube hydroforming process of a copper joint using a fuzzy controller. Int J Adv Manuf Technol 43:1–10
3. Ahmetoglu M, Altan T (2000) Tube hydroforming: state-of-the-art and future trends. J Mater Process Technol 98:25–33
4. Koc M (2008) Hydroforming for advanced manufacturing. Woodhead Publishing in Materials, New York
5. Yang J, Jeon B, Ik Oh S (2001) The tube bending technology of a hydroforming process for an automotive part. J Mater Process Technol 111:171–181
6. Nikhare C, Weiss M, Hodgson PD (2017) Buckling in low pressure tube hydroforming. J Manuf Process 28:1–10
7. Stanley P. Ash (1997) Liquid impact tool forming mold. U.S. Patent No. 5630334
8. Hedrick A (2002) The how, what, and why of liquid impact forming. STAMPING J
9. Nikhare C, Weiss M, Hodgson PD (2010) Die closing force in low pressure tube hydroforming. J Mater Process Technol 210:2238–2244
10. Huang CM, Liu JW, Zhong YZ, Wu MJ, Wang KM, Zhou RQ (2014) Exploring liquid impact forming technology of the thin-walled tubes. Appl Mech Mater 633-634:841–844
11. Hajializadeh F, Mashhadi MM (2015) Investigation and numerical analysis of impulsive hydroforming of aluminum 6061-T6 tube. J Manuf Process 20:257–273
12. Masoumi E, Ghazanfari A, Hashemi R (2013) Loading path determination for tube hydroforming process of automotive component using APDL. Int J Automot Eng 3:555–563
13. Hosseinzadeh M, Mostajeran H, Bakhshi-jooybari M, Gorji AH, Nourouzi S, Hosseinipour SJ (2009) Novel combined standard hydromechanical sheet hydroforming process. Proc Inst Mech Eng Part B 224:447–456
14. Manabe K, Amino M (2002) Effects of process parameters and material properties on deformation process in tube hydroforming. J Mater Process Technol 123:285–291
15. Koc M, Altan T (2002) Prediction of forming limits and parameters in the tube hydroforming process. Int J Mach Tool Manu 42:123–138
16. Trana K (2002) Finite element simulation of the tube hydroforming process—bending, preforming and hydroforming. J Mater Process Technol 127:401–408
17. Shi Y, Jin H, Wu PD, Lloyd DJ (2017) Effects of superimposed hydrostatic pressure on necking and fracture of tube under hydroforming. Int J Solids Struct. In press

Publisher's Note